Design of a Superconducting Magnet for the LNS Cyclotron

A. Radovinsky, L. Calabretta, J. Minervini, A. Zhukovsky, P. Michael, and A. Calanna

***Abstract*—The Massachusetts Institute of Technology has been collaborating with the Laboratori Nazionali del Sud, Istituto Nazionale di Fisica Nucleare (INFN), in Catania, Sicily, on the conceptual design of a replacement magnet for the existing LNS cyclotron used by INFN. The existing magnet was built in the early 1980s. Future nuclear physics experiments require an upgrade of the superconducting cyclotron to increase the intensity of beams by a factor of 10–100. To achieve this goal, the extraction channel through the superconducting magnet needs to be larger than the present one in both the radial and axial directions. It is for these reasons that a new superconducting magnet fitting the new requirements must be built to replace the present one. Magnetic analyses succeeded in defining a coil set satisfying the specified field form factors. Several design options were considered, including a cryostable liquid-helium-pool-cooled design, as well as several epoxy impregnated (potted) designs. The potted and helium-pooled magnet design was developed at the conceptual level. The proposed design is viable and will be used as the baseline for the next stages of the design work.**

***Index Terms*—Cyclotron, superconducting magnet.**

I. Introduction

THIS document summarizes the work done under a contract with the Laboratori Nazionali del Sud (LNS) of the Istituto Nazionale di Fisica Nucleare (INFN). The task was to propose a conceptual design of a replacement magnet for the existing LNS cyclotron used by INFN. The magnet was built in the early 1980-s and its general parameters are described in [1], [2]. The need for the upgrade was justified in [3], [4] and the requirements for the replacement magnet were specified by INFN. The magnet has to be comprised of two split pairs of solenoids called alpha and beta coils. For each of the coils the "field form factor" defined as the magnetic field calculated without iron at the mid-plane has to match that of the respective coil of the old magnet with a precision of less than 0.1%. We have to strictly satisfy this requirement only up to Rex $= 0.9$ m, the maximum beam extraction radius. The cryostat has to fit in the existing iron yoke of the old magnet. Two extreme modes have to be acceptable; Mode A with maximum same direction currents in both coil pairs; and Mode B with the maximum current in the alpha coils and maximum reverse current in the beta coils. The major reason for replacing the old magnet is that more axial space around the mid-plane is required for the new extraction channel, and consequently, the closest to the mid-plane end of the alpha coils has to be moved from Zmin $= 6.2$ cm as in the old magnet to at least Zmin $= 9.0$ cm.

TABLE I
Coil Dimensions

Coil Set	alpha	beta
Rmin [m]	1.027	1.000
Rmax [m]	1.162	1.147
Zmin [m]	0.090	0.433
Zmax [m]	0.385	0.684

Magnetic analyses succeeded in defining a coil set satisfying the field form factors with a precision of less than 0.05%. Several design options were considered, using a cryostable helium pool cooled design as well as several epoxy impregnated (potted) designs, and the preliminary winding and cable parameters were specified for each of these designs. Preliminary analyses showed that all these options appeared to be viable. Optional designs were discussed with LNS; the potted helium pooled option was selected as the baseline, primarily due to its more conventional design leading to a lower cost of manufacturing.

Following this decision the potted magnet design was developed at the conceptual level. Most attention was paid to the design and analyses of the most critical part of the superconducting magnet, its cold mass including the winding. Results of various magnetic, thermal, and structural analyses instrumental for evaluating the feasibility and critical characteristics of the magnet structure were analyzed by analytical and numerical modeling.

II. Coil Sizing and Magnet Design

A. Coil Sizing

The LNS cyclotron is designed to accelerate a variety of particle species to different energies. The isochronicity of the field profile for all these modes is provided by combining the contributions from two pairs of split coils, alpha and beta, the iron yoke and a set of 20 correction coils. At every radius the form factors of defined in Table I new coils are allowed to deviate from those of the old magnet by less than 0.1%.

Fig. 1 depicts relative field errors of the new coil set defined in Table I. They do not exceed 0.05%.

Manuscript received October 15, 2015; accepted January 20, 2016. Date of publication February 3, 2016; date of current version February 24, 2016.

A. Radovinsky, J. Minervini, A. Zhukovsky, and P. Michael are with Plasma Science and Fusion Center, Massachusetts Institute of Technology, Cambridge, MA 02139 USA (e-mail: radovinsky@psfc.mit.edu; minervini@psfc.mit.edu; zhukovsky@psfc.mit.edu; michael@psfc.mit.edu).

L. Calabretta and A. Calanna are with the Laboratori Nazionali del Sud, Istituto Nazionale di Fisica Nucleare, Catania 95123, Italy (e-mail: calabretta@lns.infn.it; calanna@lns.infn.it).

Color versions of one or more of the figures in this paper are available online at http://ieeexplore.ieee.org.

Digital Object Identifier 10.1109/TASC.2016.2525758

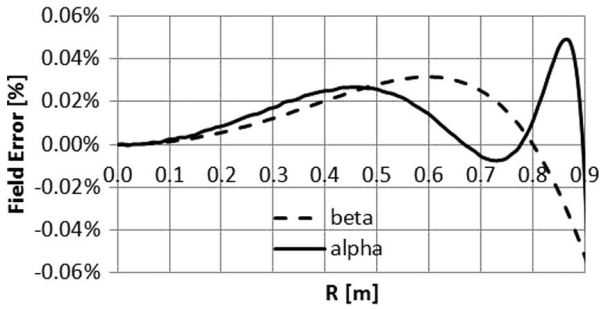

Fig. 1. Field deviations from the old form factors in alpha coil and beta coil versus radius.

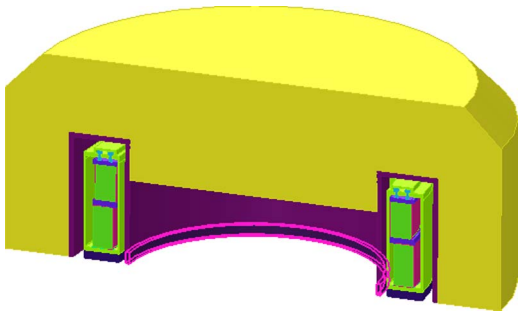

Fig. 2. One-fourth of the magnet in the iron yoke.

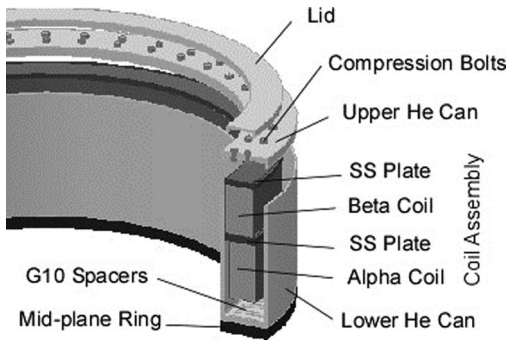

Fig. 3. Cold mass parts illustrating assembly sequence.

B. Design and Conductor Selection

Conductor was designed for a more challenging Mode A with stored energy, 55.4 MJ, about 5 T field in the beam area, peak field at the conductor of 6.1 T and engineering current density of 54 A/mm^2. At an operating current of 2 kA this corresponds to the inductance of .27.7 H. Verifying this conductor design against Mode B showed its conservative performance.

Two optional winding schemes were considered. The first one, with a cryostable helium permeated winding, is similar to that of the existing LNS magnet designed for a NbTi conductor with a reduced compared with the old design cu/sc $= 15$ ratio, the same 0.15-mm thickness of insulation and 0.2-mm per turn spacers both in radial and axial direction with the wetted fraction of the perimeter fp $= 0.6$. Its cryostability evaluated at the 2 kA operating current using Stekly criteria [5] matched its value, $\alpha_{\rm sk} = 0.8$, of the old design. This option was rejected due to the complexity of manufacturing and the cost of both the hardware and the operations.

He pool cooled potted design was chosen as the baseline, primarily due to its relative simplicity leading to a lower cost of manufacturing. The cable-in-copper-channel NbTi 4.42 mm by 7.37 mm rectangular conductor with cu/sc $= 5$ was sized for the peak field and current density in the alpha coil in Mode A at 4.2 K operating temperature, 2 kA conductor current and 2.02 K temperature margin.

Quench protection by fast discharge on an external 0.284-ohm resistor sized to limit the hot spot temperature by 155 K was evaluated using a conservative adiabatic model; the maximum terminal voltage is 570 V.

III. Cold Mass Design

A general layout of the proposed design of the magnet in a cryostat surrounded by the iron yoke is shown in Fig. 2.

The cryostat is made of the magnetic steel, s1010, except for the nonmagnetic segment of the inner diameter cylindrical wall extending from $Z = 0$ to $Z = 8$ cm. In Fig. 2 it is highlighted by a contour line.

Fig. 3 shows the cold mass. It is comprised of

— A helium can installed on the mid-plane ring, both made of stainless steel 316 (SS). Threaded holes for the tension bolts are prepared in the upper part of the helium can.

— A stacked coil assembly comprised of the alpha and beta coils, both pre-impregnated with the ground insulation, and of two SS plates, one between the coils and one on top the beta coil.

The upper part of the helium can will be welded to the cylindrical walls of the lower part of the helium can after installing the stacked coil assembly. The stacked coil assembly is installed into the helium can on top of 1-mm thick G10 spacers providing access of the coolant to the bottom of the alpha coil. The stacked coil assembly is precisely positioned coaxially to the inner wall of the helium can by (not shown here) spacers between the inner diameter of the coil assembly and the outer diameter of the inner wall of the helium can.

After welding the top of the helium can the coil assembly is axially preloaded by the compression bolts. The heads of the compression bolts are covered by a lid welded to the top of the helium can. The space under the lid is connected with the space inside the helium can by a number of holes and is also filled by liquid helium.

IV. Cold Mass Analyses

All finite element analyses were performed using Cobham Opera [6] computer program. Various combinations of analytical modules, TOSCA, a magnetostatic module; ELEKTRA, a steady state and transient electromagnetic module; TEMPO, a steady state and transient thermal module; STRESS, a steady state structural module, sometimes combined using the MULTIPHYSICS utility, were used for the analyses.

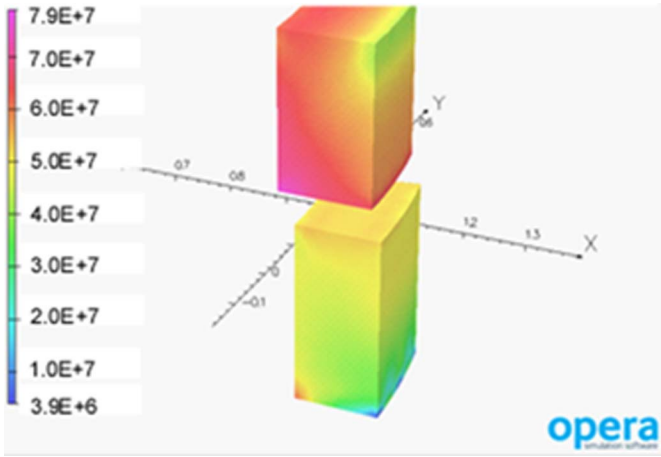

Fig. 4. Hoop stress [Pa] in the winding, mode A.

The model is shown in Fig. 2. Material properties were defined according to [7]–[10].

A. Structural Analyses

As said before in Mode B alpha and beta carry respective maximum but opposite currents. This case defines the maximum repulsion between the alpha and beta coils, which is offset by 72 25-mm bolts arranged in two evenly spaced rows as shown in Fig. 3. Structural analyses accounting for the Lorentz forces and differential thermal contraction of the helium can and the coil assembly due to the cooldown concluded that a 10.4 MN total preload will keep the coil stack in compression with a 10% margin. Assuming equal load sharing, this amounts to a 144 kN compression force per bolt. According to [11] the appropriate carbon steel bolt compression for a 1" (25.4 mm) bolt is 189 kN with respective equivalent torque of 9.62 kN.m. ASTM A307 Grade A bolts comply with this definition.

Stresses and strains in the winding pack were evaluated both for Mode B and Mode A, in which both coils carry maximum respective currents in the same direction. The winding was modeled with anisotropic thermal and structural properties. Von Mises stresses as well as hoop, radial and axial stresses were calculated and they are well within allowables. For instance, Fig. 4 shows that peak hoop stress in the modeled winding is 79 MPa. Assuming that only copper channel carries hoop forces the scaled by its fraction in the winding hoop stress in the channel is 109 MPa, which is safely below the 150 MPa allowable stress for the copper.

Stresses in the ground insulation for Modes A and B showed the maximum of 144 MPa for Von Mises Stress, the maximum of 28 MPa for tensile stress and the maximum of 110 MPa for compressive stress, all in Mode A. They are all within the allowables of G10 at 4 K.

Slip conditions at the interfaces between the windings and the SS plates were evaluated by the radial to normal pressure ratios integrated over the interface. The maximum of about a unity was observed at the interfaces at the top of alpha coil and bottom of beta coil in Mode B. Arranging slip planes between the contacting surfaces is recommended to reduce the heat deposition due to the slippage and the danger of causing the quench. For instance, reference [12] demonstrated that a bonded to the coil moderate thickness G10 plate effectively diffuses frictional heating preventing high peak temperatures from reaching the winding pack.

The helium can was structurally evaluated both at room temperature and at 4-K operating conditions for two respective combinations of loads due to the pressure drop between the liquid helium space inside the vessel and vacuum space between the outer wall of the helium can and the cryostat, loads due to the preload of the coil assembly by the compression bolts and Lorentz forces in the coils.

The number and the location of the cold-to-warm (CW) supports are defined by the penetrations in the existing iron yoke, which will be reused with the new magnet. There are 6 axial penetrations both at the top and at the bottom of the magnet, spaced by 120 degrees. They will be used for the total of 6 axial supports. The total of 6 radial supports arranged in 3 by 2 V-shaped arrangements in the mid-plane will provide the lateral support and the centering function. The V-shaped arrangement also mitigates rotation about the Z-axis.

The specific feature of a typical cyclotron design is that the coils assembled inside the cryostat magnetically interact with the ferromagnetic iron yoke. The consequence of this interaction is that one or more of the degrees of freedom of the cold mass is magnetically unstable. This magnetic instability has to be offset by the exceeding mechanical stiffness of the CW support elements. At the same time, the axial CW supports have to be designed to carry the weight of the cold mass.

Electromagnetic modeling showed that forces and moments due to magnetic stiffness are practically linear functions of respective offsets,

- Destabilizing linear axial stiffness is 16.2 MN/m
- Destabilizing rotational tilt stiffness is 15.4 MN.m/rad
- Stabilizing linear lateral stiffness is 8.0 MN/m.

For the purposes of the initial sizing we assume that all CW support tension links are made of Navtec N-50 Nitronic rods.[1] Analyses showed that any Navtec N50 rods starting with R505-017 qualify for the axial supports and that the thinnest, $D = 4.37$ mm rods R505-004 can be used for the radial supports.

And finally, the impact of the coil deformations in the area of the extraction channel cutout in the mid-plane ring on the quality of the magnetic field in the beam acceleration space was evaluated for Mode A. Analyses indicated a 0.15-mm sagging at the bottom of alpha coil and practically no distortion of the axisymmetric axial field component at the extraction radius, Rex $= 0.9$ m.

B. Cryogenics

Requirements to the cryogenic system were specified in terms of maximum consumption of the coolants, 20 l/hr of helium at 4 K and 18 l/hr of LN2 at 77 K, which (by the enthalpy

[1]http://www.navtec.net/products.asp?id=53&type=16&channel=1

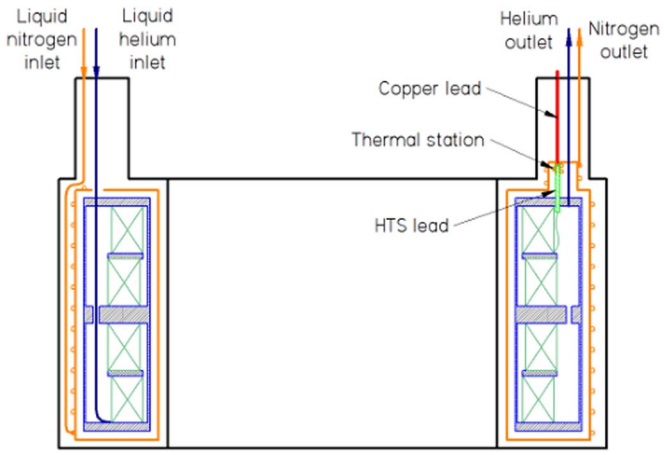

Fig. 5. Cooling scheme.

of vaporization) translates into 14.4 W and 805 W of heat loads at respective stages.

The cooling scheme of the magnet is shown in Fig. 5. The upper and lower sets of alpha and beta coils are placed, respectively in closed, annular vessels located symmetrically about the mid-plane of the cyclotron.

Both sets of alpha and beta coils are cooled by immersion in boiling liquid helium bath at atmospheric pressure. The liquid is introduced by a transfer syphon directly connected to the lower magnet vessel, the one below the cyclotron mid-plane. Overflow from the lower magnet vessel is used to fill the magnet vessel, the one above the cyclotron mid-plane. The magnet vessels are connected across the cyclotron mid-plane by tubes that allow for helium filling from the lower to upper magnet vessel and provide access for instrumentation and magnet lead wires, which exit the cryostat through service chimneys projecting upward from the top of the cryostat. The cryogen fill and vent lines are similarly directed to a service cryostat through one of the three service chimneys at the top of the cryostat.

Current leads protruding from the ends of the coils are directed to a set of hermetic feedthroughs mounted to the top plate of the upper magnet vessel where they connect to high temperature superconductor current leads, which span the gap between the upper magnet vessel and a liquid nitrogen cooled thermal station, where they connect to conduction cooled copper leads which complete the link to room temperature. The instrumentation lead wires similarly exit the magnet vessel through hermetic connectors mounted to the top plate of the upper magnet vessel. The instrumentation wires are similarly heat sunk to a liquid nitrogen cooled thermal anchor before continuing out of the cryostat through one of the service chimneys.

The cold mass is surrounded by an aluminum radiation shield, which is cooled by a forced flow of boiling liquid nitrogen in the tracers located at both the inner and outer surfaces of the radiation shield. All cold surfaces are covered with Al foil to reduce radiation heat loads. The radiation shield is covered with multilayer insulation (MLI) to reduce a heat flux from the room temperature walls of the solenoid vacuum vessel.

TABLE II
HEAT LOAD TO LIQUID HELIUM

Heat load source	Heat load, W
Radiation from the shield with 100% margin	1.0
Convection of residual helium gas	0.3
Conduction along support rods	0.3
Conduction along instrumentation wires	0.25
Heat leak through 4 HTS current leads	1.92
Heat dissipation in 8 x 2 joints	0.32
Nuclear Heating	2.0
Total heat load to liquid helium	6.09

TABLE III
HEAT LOAD TO LIQUID NITROGEN

Heat load source	Heat load, W
Radiation through MLI with 100% margin	40
Thermal conduction along support rods	6
Heat load through 4 current leads	340
Total heat load to liquid nitrogen	386

Two pairs of 2 kA current leads are considered for both alpha and beta coils circuits bringing the total number of the current leads to four. Each of the leads is comprised of a room temperature (300 K) to intermediate (77 K) temperature optimized [13] copper wire and a high temperature superconductor (HTS) lead between the intermediate temperature intercept and the 4 K end.

Tables II and III show itemized heat loads at both stages.

They comprise less than half of the respective liquid helium and liquid nitrogen specs. The remaining margin will be partially used to compensate losses in the transmission lines and in the helium liquefier.

V. CONCLUSION

Magnetic analyses succeeded in defining a coil set satisfying the field form factors with a precision of less than 0.05%. Several design options were considered including a cryostable liquid helium pool cooled design, as well as several epoxy impregnated (potted) designs. The potted helium pooled magnet design was developed at the conceptual level. Results of various magnetic, thermal, and structural analyses instrumental for evaluating the feasibility and critical characteristics of the magnet structure indicate that the proposed design is viable and can be used as the baseline for the next stages of the design work.

REFERENCES

[1] E. Acerbi, F. Alessandria, G. Baccaglioni, and L. Rossi, "Design of the Main Coils for the Milan Superconducting Cyclotron," in *Proc. 9th Int. Conf. Cyclotrons Appl.*, Caen, France, Sep. 1981, pp. 399–401.
[2] E. Acerbi *et al.*, "The Milan superconducting cyclotron project," in *Proc. 9th Int. Conf. Cyclotrons Appl.*, Caen, France, Sep. 1981, pp. 169–176.
[3] A. Calanna *et al.*, "Upgrade of the LNS Superconducting Cyclotron," presented at the 6th Int. Particle Accelerator Conf., Richmond, VA, USA, Apr. 2015, Paper THPF037. [Online]. Available: http://accelconf.web.cern.ch/AccelConf/IPAC2015/papers/thpf037.pdf
[4] A. Calanna *et al.*, "Proposal to increase the extracted beam power from the LNS-INFN superconducting cyclotron," presented at the 13th Int. Conf. Heavy Ion Accelerator Technology, Yokohama, Japan, Sep. 2015, Paper MOA1C03.
[5] M. Wilson, "Stabilization of superconductors for use in magnets," *IEEE Trans. Magn.*, vol. MAG-13, no. 1, pp. 440–446, Jan. 1977.

[6] Cobham Opera, Computer Program. [Online]. Available: http://www.cobham.com
[7] S. Chattopadhyay, *Pressure Vessels: Design and Practice*. Boca Raton, FL, USA: CRC Press, 2005.
[8] Young's Modulus vs Temperature Chart. [Online]. Available: http://www.copper.org/resources/properties/cryogenic/homepage.html
[9] J. W. Sa *et al.*, "Mechanical characteristics of austenitic stainless steel 316LN weldments at cryogenic temperature," in *Proc. 21st IEEE/NPS Symp. Fusion Eng.*, Sep. 2005, pp. 1–4.
[10] NIST Material Properties. [Online]. Available: http://cryogenics.nist.gov
[11] K. Lingaiah-Machine, *Design Handbook*. 2nd ed. New York, NY, USA: McGraw-Hill, 2003, p. 517.
[12] Y. Iwasa *et al.*, "The effect on stability of frictional decoupling for a composite superconductor," in *Proc. 8th Symp. Eng. Probl. Fusion Res.*, 1979, pp. 1407–1411.
[13] R. McFee, "Optimum input leads for cryogenic aparatus," *Rev. Sci. Instrum.*, vol. 30, no. 2, pp. 98–102, Feb. 1959.